Liquid Crystals
Publication details, including instructions for authors and subscription information:
http://www.tandfonline.com/loi/tlct20

Analysis of focal length of blue-phase liquid crystal (BPLC) cylindrical lens for the light of the various incident angles and polarisations

Hyungki Hong [a]

[a] Department of Optometry, Seoul National University of Science and Technology, Seoul, Republic of Korea

Version of record first published: 09 Jan 2013.

To cite this article: Hyungki Hong (2013): Analysis of focal length of blue-phase liquid crystal (BPLC) cylindrical lens for the light of the various incident angles and polarisations, Liquid Crystals, 40:4, 450-457

To link to this article: http://dx.doi.org/10.1080/02678292.2012.757371

Liquid Crystals, 2013
Vol. 40, No. 4, 450–457, http://dx.doi.org/10.1080/02678292.2012.757371

Taylor & Francis
Taylor & Francis Group

Analysis of focal length of blue-phase liquid crystal (BPLC) cylindrical lens for the light of the various incident angles and polarisations

Hyungki Hong*

Department of Optometry, Seoul National University of Science and Technology, Seoul, Republic of Korea

(*Received 24 September 2012; final version received 6 December 2012*)

Horizontally non-uniform electric field along the vertical direction inside blue-phase liquid crystal (BPLC) layer induces the Gradient index (GRIN) lens effect. Dependence of lens performance on the incident angle and polarisation is investigated by calculating the spatial phase distribution and the direction of wave front for lights passing through the BPLC layer. The calculated trajectories of light rays show that the focal distance for e-wave is less affected by the incidence angle than the focal distance of the o-wave. This can be attributed to the fact that steepness of spatial distribution of the effective refractive index for e-wave decreases for the larger incident angles.

Keywords: blue-phase liquid crystal; Gradient index lens; polarisation; incident angle

1. Introduction

Gradient index (GRIN) lens using liquid crystal (LC) material had been reported where the spatially non-uniform electric fields induce the spatially non-uniform distribution of the LC directors [1–3]. This technique can control the lens effect electrically. Performance of this lens such as focal length and polarisation dependency is related to the anisotropic characteristics of LC material used for GRIN lens.

Recently, polymer-stabilised blue-phase liquid crystal (BPLC) had been reported where the uniaxial state of BLPC can be stably induced under the electric field at the wide temperature range [4,5]. Refractive indices of the uniaxial medium are characterised by two parameters, n_o and n_e. In case of BPLC, these refractive indices are determined by the intensity of the electric field and the sign of the dielectric anisotropy [6,7]. When the dielectric anisotropy of BPLC is positive, the optic axis of BPLC is induced parallel to the direction of the electric field [6]. For the optical devices using BPLC, the configurations of the various electrode structures had been reported for the applications such as the display, the grating and the lens [8–13]. While BLPC under the electric field is uniaxial, polarisation independency of BPCL grating and lens had been reported for some of these configurations [9–13]. However, this polarisation independency is valid only for the special cases that the propagation of the incident light is parallel to the optic axis of BPLC. Hence, more investigation is needed to characterise the dependence of the optical device using BPLC on the polarisation and the incidence angle.

In this paper, dependence of the characteristics of cylindrical GRIN lens using BPLC on the polarisation and the incidence angle is investigated. For this purpose, the spatial phase distribution induced by the BPLC is determined for the various incident angles for the o-wave and e-wave. Then, the direction of the wave front and the ray trajectories are determined from these spatial phase distribution. How the light rays gathers around a point, is used to characterise the focus and the aberrations of the lens.

2. Background

BPLC material is the isotropic state under zero electric field and the refractive index can be represented as n_{iso}. And optical characteristic of BPLC becomes uniaxial under the electric field. The refractive index of BPLC at the uniaxial state under the non-zero electric field can be represented as $n_o = n_{iso} - \Delta n_{ind}(E)/3$ and $n_e = n_{iso} + 2\Delta n_{ind}(E)/3$, respectively, where $\Delta n_{ind}(E)$ is determined by the characteristics of each BPLC material [14]. When the dielectric anisotropy of BPLC is positive, the optic axis of BPLC becomes parallel to the direction of the electric field as illustrated in Figure 1(a). On the other hand, the optic axis of BLC becomes perpendicular to the direction of the electric field for BPLC of the negative Kerr constant [7].

Figure 1(b) illustrates the working principle of the lens using BPLC based on the GRIN effect. When the vertical electric field of the spatially non-uniform intensity is applied to the BPLC cell, these electric fields induce the spatial non-uniform distribution of n_o and n_e, where the optic axis of BPLC is along the vertical direction.

When the light propagates inside non-isotropic medium, the light can be treated as the combination

*Email: hyungki.hong@snut.ac.kr

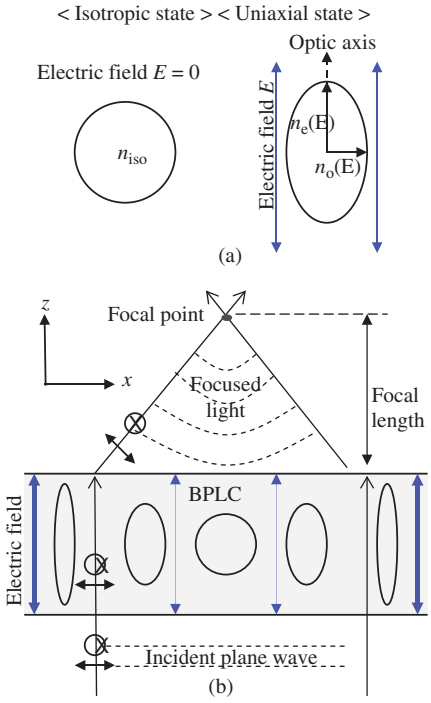

Figure 1. (a) Blue-phase liquid crystal (BPLC) of the positive dielectric anisotropy in the isotropic state under zero electric field and the uniaxial state under non-zero electric field E. (b) GRIN lens of BPLC induced by the horizontally non-uniform electric field which caused the optic axis of BPLC along the vertical direction.

of two polarisations, o-wave and e-wave. The refractive indices of o-wave and e-wave are n_o and the effective refractive index n_{eff}, respectively. When the incident light is along the z-axis of Figure 1(b), the optic axis of BLPC is parallel to the direction of the propagating light. If the direction of the incident light is parallel to the optic axis of the uniaxial medium, n_{eff} becomes the same as n_o. Hence, for this incident direction, the refractive index for o-wave and e-wave becomes the same. If the lens is thin enough that the change of light trajectory inside BPLC medium is negligible, the lens function of this structure becomes polarisation independent. The reported polarisation independences are based on this condition that the optic axis of BPLC is parallel to the direction of the propagating light [9–11,13].

But when the incident light direction is not parallel to the optic axis of BPLC, the value of n_{eff} is affected by the incident direction as illustrated in Figure 2. The effective refractive index n_{eff} can be determined by n_o, n_e and the angle θ between the optic axis and the propagating direction of light incident angle. As the refractive indices are different for the o-wave and e-wave of the oblique incidence, the lens effect is also expected to be different for the o-wave and e-wave for the oblique incidence.

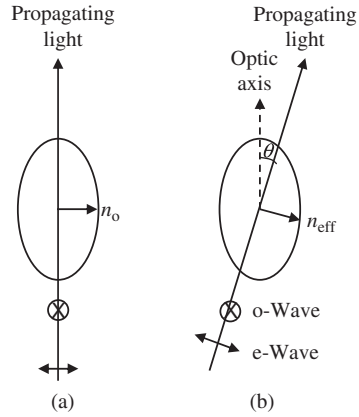

Figure 2. Refractive index of o-wave and e-wave of BPLC of the uniaxial state where the directions of the propagating lights are (a) parallel to the optic axis of BPLC and (b) not parallel.

3. Simulation

To calculate the spatial phase distribution induced by BLPL lens, a configuration of cylindrical lens with lens pitch of 0.2 mm is assumed. The direction of the infinite radius of cylindrical lens is selected to be along the y-direction as illustrated in Figure 3(a). The incident light is selected to be on the zx-plane and the direction of the normal incidence is parallel to the z-axis. A simplified BPLC cell structure is assumed such that the spatial distribution of n_o and n_e are uniform along the direction of z-axis.

In case of the configuration of Figure 3(a), the angle θ defined in the Figure 2 is equal to the refracted angle θ_r. Using the Snell's law of $n_{eff} \sin \theta_r = \sin \theta_{in}$, the effective refractive index n_{eff} of BPLC can be written as the function of the incident angle θ_{in}.

$$n_{eff}^2 = n_o^2 + \left(1 - \frac{n_o^2}{n_e^2}\right) \sin^2 \theta_{in} = n_{iso}^2 \left(1 - \Delta n_{ind}/3\right) + \frac{(2 + \Delta n_{ind})\, \Delta n_{ind}/3}{(1 + 2\Delta n_{ind}/3)^2} \sin^2 \theta_{in} \quad (1)$$

In case of the selected configuration, n_{eff} is equal to n_o at the incident angle of $\theta_{in} = 0°$. At $\theta_{in} = 90°$, the refractive angle θ_r is less than 90° by the Snell's law and n_{eff} is always smaller than n_e. BPLC lens with cell gap of a few tens of micrometres, $\Delta n_{ind}(E)$ of around 0.1 and the positive dielectric anisotropy had been reported [13,15]. Based on this information of BPLC material and the lens design, two conditions of BPLC lens configuration are investigated. One condition that the thickness of BPLC cell is 13 μm, $\Delta n_{ind}(E)$ is 0.06 and focal length is 19 mm, corresponds to the reported structure. And the focal length for this condition is more than thousand times larger than

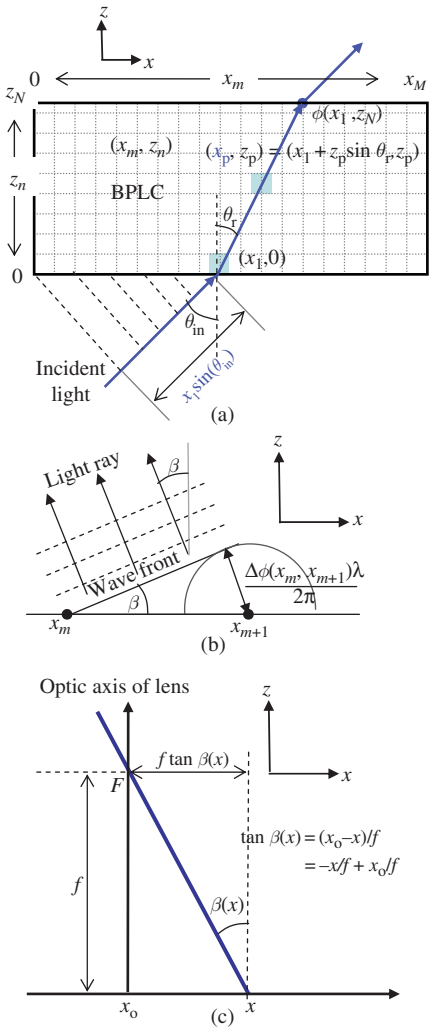

Figure 3. (a) Propagation of light through BPLC medium which is treated as M by N meshes. (b) Determination of the light ray direction from the phases at the two adjacent position x_m and x_{m+1} and the wave front. (c) Relation between the focal position F and the light ray of the direction β. Lens is located on the x-axis.

the thickness of BPLC cell. The other condition that the thickness of BPLC cell is 50 μm, $\Delta n_{ind}(E)$ is 0.12 and focal length is 2.5 mm is also considered to investigate the characteristics of the lens performance when the focal length is smaller than hundred times the thickness of BPLC cell. These two conditions are summarised in Table 1.

Table 1. Configurations condition of cylindrical BPLC GRIN lens.

	Thickness of BPLC (μm)	$\Delta n_{ind}(E)$	Focal length (mm)
Condition 1	13	0.06	19
Condition 2	50	0.12	2

Spatial phase distribution of n_o is selected such that the phase distribution induced by BPLC lens for the normally incident light is parabolic. For the parabolic profile, the incident lights parallel to the optic axis will be focused to a single position. Hence, for the incident light parallel to the optic axis, the spherical aberration is known to be prevented [16].

The light path for the obliquely incident light through BPLC layers are illustrated in Figure 3(a). In case of the normal incidence that the plane wave is incident on the lower side of the substrate, the phase for the wave front is the same irrespective of the horizontal position. And x-coordinate of the light path remains the same inside BPLC layer. However, when the plane wave of the incident angle θ_{in} is incident on the lower side of the substrate, the phases for the wave front are different by the amount of $kx_1\sin(\theta_{in})$ where the horizontal position x_1 is the position that the light ray enters LC cell [17]. And the x-coordinate of the light path inside BPLC layer becomes $x_1 + z\ \sin(\theta_r)$, where θ_r is the refractive angle. Phase difference of the incident wave front and the phase induced by BPLC should be together considered in calculating the phase profile of BPLC lens for the oblique incidence.

Directional dependence for the e-wave and o-wave is investigated by treating the BPLC cell as M by N meshes where each mesh is considered as the uniform uniaxial medium. BPLC cell is treated as the combination of N layer with thickness $(z_N)/N = \Delta z$, where thickness of LC cell gap is z_N, When the light of the incident angle θ_{in} is incident at the position of $(x_1, 0)$ on the side of the lower substrate, the coordinate (x_p, z_p) of the light path at pth layer along the z-direction can be written as follows:

$$x_p = x_1 + z_p\sin(\theta_r) = x_1 + p\Delta z\ \sin(\theta_r) \qquad (2)$$

So Equation (1) can be used to determine the effective refractive index n_{eff} at the different positions and the refractive angle θ_r can be derived from the incident angle θ_{in} by the Snell's equation. Phase change by the mesh of the position (x_p, z_p) can be written in Jones matrix representation as follows [18]:

$$M(x_1, x_p, z_p) = \boldsymbol{R}(-\phi_2(x_p, z_p))\boldsymbol{P}(x_p, z_p)\boldsymbol{R}(\phi_2(x_p, z_p)) \quad (3)$$

where ϕ_2 represents the azimuth angle of the optical axis of BPLC. $\boldsymbol{R}$ represents rotation matrix $\boldsymbol{R}$ and propagation matrix $\boldsymbol{P}$ is represented as

$$P(x_p, z_p) = \begin{pmatrix} \exp\left(-i\frac{2\pi\Delta z \cdot n_o}{\lambda}\right) & 0 \\ 0 & \exp\left(-i\frac{2\pi\Delta z \cdot n_{eff}(x_1, x_p, z_p)}{\lambda}\right) \end{pmatrix} \quad (4)$$

and λ represents the wavelength. Phase induced by BPLC medium along the light path can be determined by the successive matrix multiplication of Jones matrix representation as follows:

$$M(x_1) = \sum_{z_p=0}^{z_N} M(x_1, x_p, z_p) \tag{5}$$

From Equations (4) and (5), phase distribution by BPLC lens can be calculated for the x-coordinate x_1 which is the position that the light ray enters LC cell. Phase difference $kx_1\sin(\theta_{in})$ of the incident wave front should be also included in the calculation of the overall phase change.

Ray trajectories can be estimated from the phase between the two adjacent positions as illustrated in Figure 3(b) [17]. BPLC lens induces the spatially non-uniform phase profile. When the phase difference between two positions x_m and x_{m+1} is $\Delta\phi(x_m, x_{m+1})$, a position that is distant from x_{m+1} by $\Delta\phi(x_m, x_{m+1})/k = \Delta\phi(x_m, x_{m+1})\lambda/2\pi$ will have the same phase as position x_m. From these positions of the same phase, the wave front which has the same phase can be determined. And the light propagates perpendicular to the wave front. In Figure 3(b), angle β that represents the propagating direction of the wave front can be determined from the following equation.

$$\beta(x_m, x_{m+1}) = \sin^{-1}\left(\frac{\Delta\varphi\,(x_m, x_{m+1})}{x_{m+1} - x_m}\frac{\lambda}{2\pi}\right) \tag{6}$$

Hence, the directions of light rays coming out from the BPLC lens can be determined from Equation (6). Figure 3(c) illustrates the path of the light ray where the lens is located on positions of $z = 0$ and the optic axis of the lens pass through x_0. In case of the ideal lens, all light rays should pass through on a specific position on the optic axis of the lens irrespective of the positions that light rays are incident on the lens. This position F can be defined as the focus of the lens. As the tangent of angle $\beta(x)$ corresponds to the inverse of the focal distance, the following equation can be derived.

$$\tan\beta(x) \propto -x/f \tag{7}$$

Equation (7) can be used to determine the focal distance from the ray direction.

4. Result and analysis

Figure 4 illustrates how the effective refractive index n_{eff} changes at the various incident angles for the different n_o values. These results are derived from Equation (1). In Figure 4, n_{eff} becomes larger than n_o as the incident angle increases. n_{eff} approaches n_{iso} as the refractive angle is beyond 70°. For the obliquely incident light, the steepness of the curves of Figure 4 decreases.

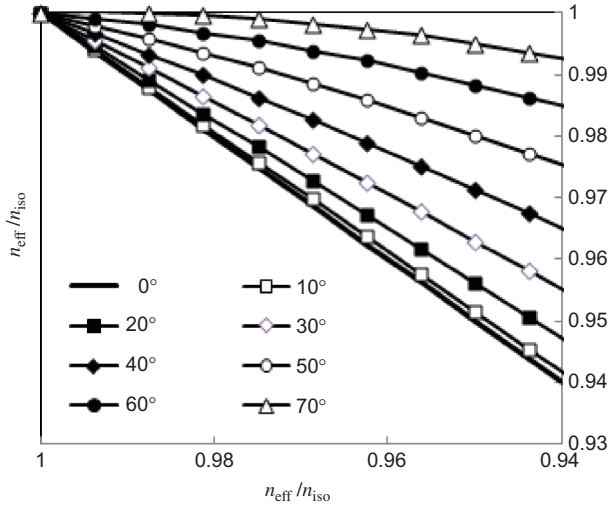

Figure 4. Effective refractive index n_{eff} of e-wave at the various incidence angles. The horizontal and the vertical axes represent n_{eff}/n_{iso} and n_o/n_{iso}, respectively. Numbers on the lower left side represent the incidence angles.

Figure 5 illustrates the calculated phase distribution induced by BPLC layer of GRIN lens for o-wave and e-wave for the condition 1. Figure 5 shows the noticeably different trend of the phase distribution for e-wave and o-wave. In Figure 5(b), the spatial steepness of phase distribution curve for e-wave decreases noticeably as the incident angle increases. This can be attributed to the fact that n_{eff} changes towards n_{iso} and the steepness decreases for the larger incident angle as illustrated in Figure 4.

Figure 6 illustrates the tangent of the propagating directions of light rays determined from the result of Figure 5 and the procedure described in Figure 3(b). Figure 6 also illustrates the result of the linear fitting curve. In Figure 6, the tangent values match the linear fitting curve with R^2 value of larger than 0.999 for the incident angles of the range between 0° and 40°. It means that the parabolic phase distribution characterising the focus is still conserved for the oblique incident light for the lens configuration of condition 1. Focal distance can be determined from the inverse of the tangent angle of the linear fitting curve as illustrated in Figure 3(c) and Equation (7). The calculated focal distance for the various incident angles at condition 1 are derived and listed in Table 2.

For the condition 2, where the cell thickness is much larger than that of the condition 1, the calculated phase distribution, the directions of the propagating

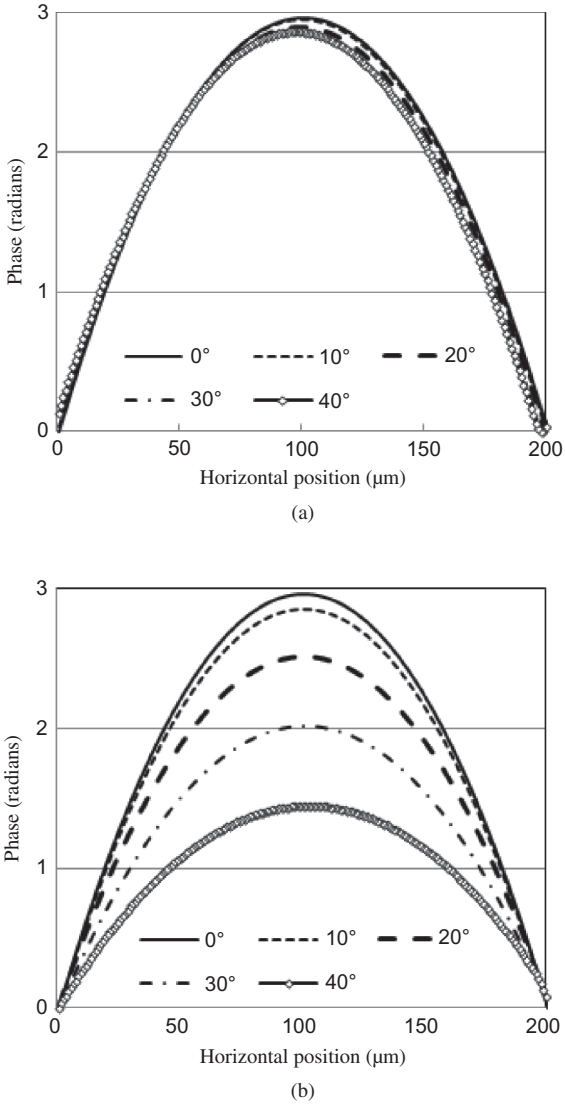

Figure 5. Calculated phase distribution induced by BPLC layer of GRIN lens at the condition 1 of Table 1 for (a) o-wave and (b) e-wave. The horizontal and the vertical axes represent the horizontal position of the lens and the phase, respectively. Numbers on the lower side represent the incidence angles.

Table 2. Calculated focal distances for o-wave and e-wave at the condition 1 of Table 1.

Incident angle (°)	o-Wave (mm)	e-Wave (mm)
0	19.2	19.2
10	18.4	19.1
20	16.3	18.9
30	12.9	18.6
40	8.8	18.5

light and the focal distance F are determined by the same procedure. Tangent angle of the propagating direction for the condition 2 was calculated to be

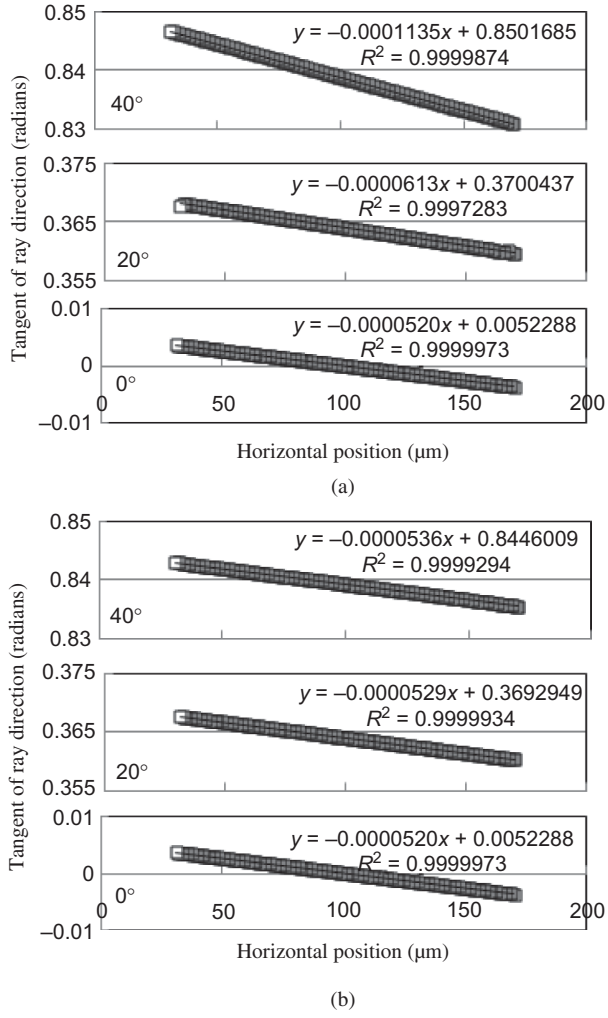

Figure 6. Tangent of the direction of light rays calculated at the condition 1 of Table 1 and the fitting curve of these results for (a) o-wave and (b) e-wave. The horizontal axis represents the horizontal position of the lens. Numbers on the lower left side represent the incidence angles.

linear and R^2 value of the linear fitting curve was larger than 0.999 for the incident angle of the range between 0° and 40°. The calculated focal distances for the condition 2 are listed in Table 3.

Results of the linear fitting curve for the conditions 1 and 2 imply that the parabolic shape of the

Table 3. Calculated focal distances for o-wave and e-wave at the condition 2 of Table 1.

Incident angle (°)	o-Wave (mm)	e-Wave (mm)
0	2.50	2.50
10	2.40	2.49
20	2.12	2.44
30	1.69	2.39
40	1.17	2.34

phase distribution is conserved even for the oblique incidence. This can be attributed to the fact that the directional dependence of n_{eff} is almost linear as illustrated in Figure 4.

Figure 7 illustrates the focal distance normalised to 1 for the condition 1 and condition 2. Focal distance for condition 1 is about 10 times larger than that for condition 2, but the directional dependences show the similar trends for conditions 1 and 2. As the incident angle increases, the focal distance for o-wave decreases noticeably, while the focal distance for e-wave remains almost unchanged.

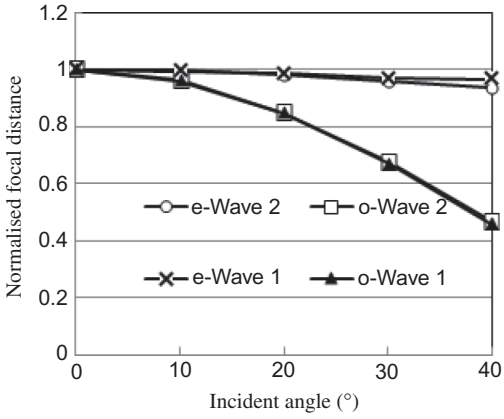

Figure 7. Normalised focal distances for the various incident angles. The horizontal axis represents the incident angles. 1 and 2 at the end of e-wave and o-wave notations represent the conditions 1 and 2 of Table 1.

Figure 8 illustrates that ray trajectories on the *xz*-plane for o-wave and e-wave at the condition 1. Ray trajectories gather around a specific position at each incident angle. These positions are notified by the circles and accord with the result of the calculated focal distance of Table 2. Figure 9 illustrates that ray trajectories on the *xz*-plane for o-wave and e-wave at the condition 2. Positions that ray trajectories gather at each incident angle are notified by the circles. While the focal distance for the condition 1 is about 10 times larger than that of condition 2, similar directional dependences are observed for the o-wave and e-wave, respectively.

Figure 10 illustrates the schematic diagram of the light trajectories by the ideal lens for the obliquely incident light. When the focused image appears on the plane located at the distance of f for the light of the incident angle β, light passing through the centre of the lens should ideally focus on the position F' which is distant from F by the amount of $f \tan \beta$. Here β represents the incident angle β with respect to the optical axis of the lens. When light rays do not focus on F', this will result in the degradation of the lens performance. This aberration which occurs for the incident light unparallel to the optic axis of the lens is called Coma

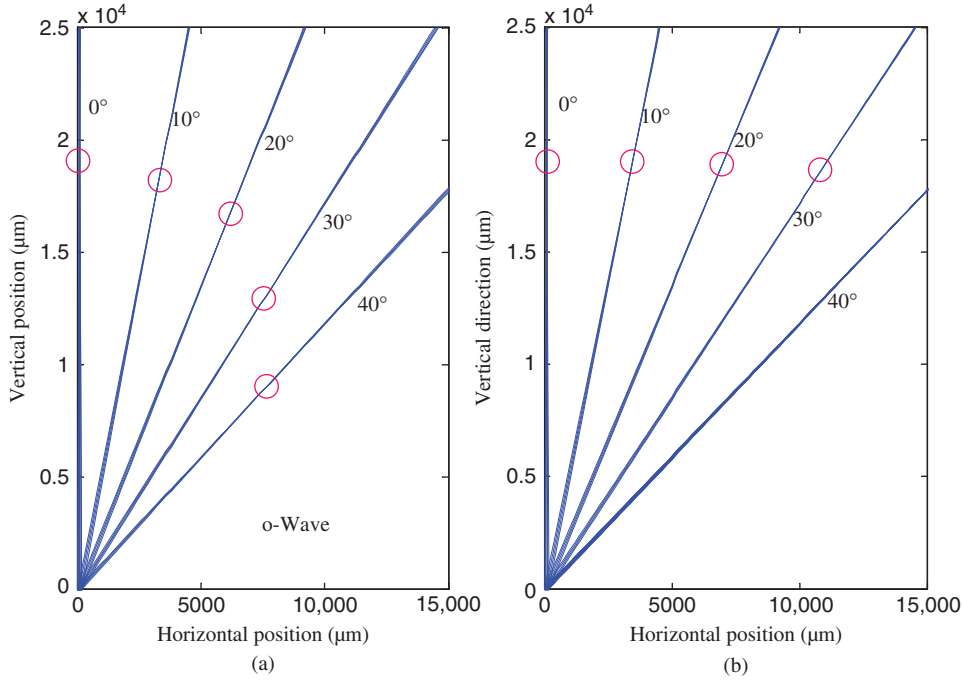

Figure 8. Ray trajectories on the *zx*-plane for the light passing through BPLC lens for the incident angles between 0° and 40° at condition 1 for (a) o-wave and (b) e-wave. Lens is located near the lower left corner of each graph. The positions that light rays focus are noted by circles. Vertical direction is parallel to the optics axis of lens.

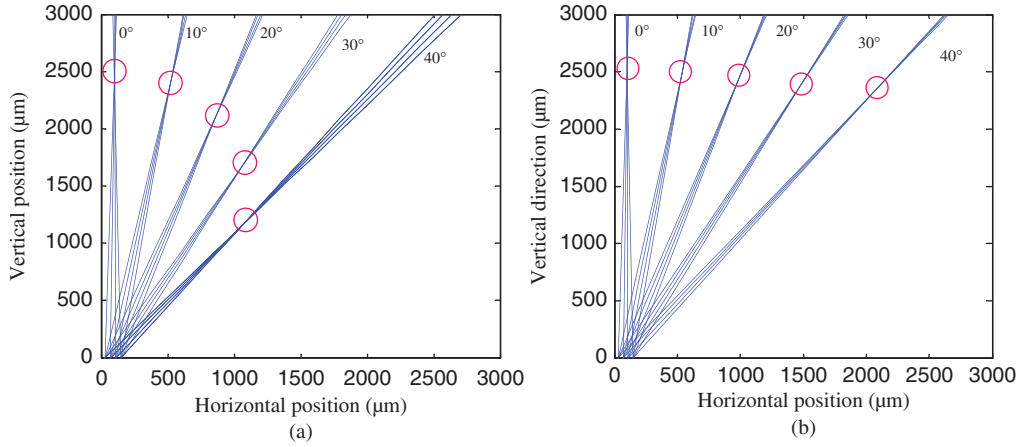

Figure 9. Ray trajectories on the *zx*-plane for the light passing through BPLC lens for the incident angles between 0° and 40° at condition 2 for (a) o-wave and (b) e-wave. Lens is located near the lower left corner of each graph. The positions that light rays focus are noted by circles. Vertical direction is parallel to the optics axis of lens.

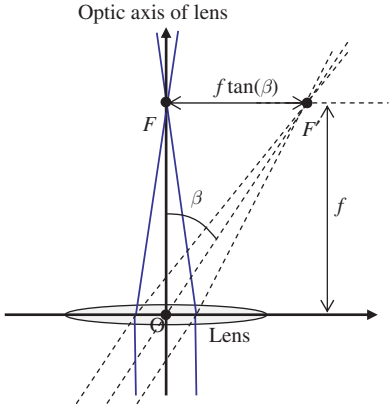

Figure 10. Schematic diagram of focus of lens for the normally and the obliquely incident light. When there is no Coma aberration, the focal distance f is not changed for the obliquely incident light.

aberration [19]. Directional dependence of GRIN lens using BPLC is different for the polarisations of o-wave and e-wave. The result of o-wave can be considered to be similar to the lens of the isotropic medium as the refractive index is not affected by the incident angles. Focusing characteristics of BPLC lens show a quite smaller aberration for e-wave compared with o-wave. When there is no Coma aberration, the length of OF' is longer than the length of OF by the factor of $1/\tan\beta$ as illustrated in Figure 10. It means that the steepness of the lens profiles should decrease in order that the obliquely incident lights focus on F'. For the larger incident angle, the effective refractive index n_{eff} of e-wave changes towards n_{sio} and steepness of phase distribution decreases accordingly as illustrated in Figure 4. Such a directional dependence of n_{eff} in BPLC lens of the given configuration seems to be the cause to focus the light of e-wave at the same distance f and reduce the Coma aberration.

5. Conclusion

Lens effect of cylindrical GRIN lens by BPLC of the vertically aligned optic axis is reported to be independent of the polarisation for the normally incident light. But at the oblique incidence, the refractive index for o-wave and e-wave becomes different and this results in the polarisation dependency of the lens characteristics such as focal distance. Focal distance of BPLC lens for o-wave decreases for the obliquely incident light. However, the lens characteristics for e-wave show the tendency of the mostly constant focal distance and the reduced Coma aberration. This can be attributed to the direction dependence of n_{eff} of BPLC such that the steepness of spatial distribution of n_{eff} decreases for the larger incident angle.

Acknowledgement

This study was financially supported by Seoul National University of Science & Technology.

References

[1] Kowel ST, Cleverly DS, Kornriech PG. Focusing by electrical modulation of refraction in a liquid crystal cell. Appl Opt. 1984;23:278–289.
[2] Ye M, Sato S. Optical properties of liquid crystal lens of any size. Jpn J Appl Phys. 2002;41:L571–L573.
[3] Hong HK, Jung SM, Lee BJ, Shin HH. Electric-field-driven LC lens for 3-D/2-D autostereoscopic display. J SID. 2009;17:399–406.
[4] Kikuchi H, Yokota M, Hiskado Y, Yang H, Kajiyama T. Polymer-stabilized liquid crystal blue phases. Nat Mater. 2002;1:64–68.

[5] Hisakado Y, Kikuchi H, Nagamura T, Kajiyama T. Large electro-optic Kerr effect in nanostructured chiral liquid crystal composites over a wide temperature range. Adv Mater. 2005;17:2311–2315.
[6] Rao L, Ge Z, Wu ST. Viewing angle controllable displays with a blue-phase liquid crystal cell. Opt Express. 2010;18:3143–3148.
[7] Li Y, Chen Y, Yan J, Liu Y, Cui J, Wang Q, Wu ST. Polymer-stabilized blue phase liquid crystal with a negative Kerr constant. Opt Mater Express. 2012;2: 1135–1140.
[8] Ge Z, Gauza S, Jiao M, Xianyu H, Wu ST. Electro-optics of polymer-stabilized blue phase liquid crystal displays. Appl Phys Lett. 2009;94:101104.
[9] Lin YH, Chen HS, Lin HC, Tsou YS, Hsu HK, Li WY. Polarizer-free and fast response microlens arrays using polymer-stabilized blue phase liquid crystals. Appl Phys Lett. 2010;96:113505.
[10] Li Y, Wu ST. Polarization independent adaptive microlens with a blue-phase liquid crystal. Opt Express. 2011;19:8045–8050.
[11] Lee CT, Li Y, Lin HY, Wu ST. Design of polarization-insensitive multi-electrode GRIN lens with a blue-phase liquid crystal. Opt Express. 2011;19:17402–17407.
[12] Zhu G, Li J, Lin Z, Wang H, Zheng Z, Cui H, Shen D, Lu Y. Polarization-independent blue-phase liquid-crystal gratings driven by vertical electric field. J SID. 2012;20:341–346.
[13] Li Y, Liu Y, Li Q, Wu ST. Polarization independent blue-phase liquid crystal cylindrical lens with a resistive film. Appl Opt. 2012;51:2568–2572.
[14] Yan J, Rao L, Jiao M, Li Y, Cheng HC, Wu ST. Polymer-stabilized optically isotropic liquid crystals for next-generation display and photonics applications. J Mater Chem. 2011;21:7870–7877.
[15] Yan J, Chen HC, Gauza S, Li Y, Meizi J, Rao L, Wu ST. Extended Kerr effect of polymer-stabilized blue-phase liquid crystals. Appl Phys Lett. 2010;96:071105.
[16] Fowles GR. Introduction to modern optics. New York: Holt Rinehart and Winston, Inc.; 1975.
[17] Hong HK. Analysis of the performance of the electric-field-driven liquid crystal lens (ELC Lens) for light of various incident angles. Liq Cryst. 2012;39: 1055–1061.
[18] Yang DK, Wu ST. Fundamentals of liquid crystal devices. Chichester: Wiley; 2006.
[19] Jenkins FA, White HE. Fundamental of optics. London: McGraw-Hill; 1981.